

Article

Collider Searches for Dark Matter (ATLAS + CMS)

Nicolò Trevisani  on Behalf of the ATLAS and CMS Collaborations

Instituto de Física de Cantabria, Universidad de Cantabria, 39005 Santander, Spain; nicolo.trevisani@cern.ch

Received: 5 November 2018; Accepted: 15 November 2018; Published: 20 November 2018

Abstract: Several searches for dark matter have been performed by the CMS and ATLAS collaborations, using proton-proton collisions with a center-of-mass energy of 13 TeV produced by the Large Hadron Collider. Different signatures may highlight the presence of dark matter: the imbalance in the transverse momentum in an event due to the presence of undetectable dark matter particles, produced together with one Standard Model particle, a bump in the di-jet or di-lepton invariant mass distributions, or an excess of events in the di-jet angular distribution, produced by a dark matter mediator. No significant discrepancies with respect to the Standard Model predictions have been found in data, so that limits on the dark matter couplings to ordinary matter, or limits on the dark matter particles and mediators masses have been set. The results are also re-interpreted as limits on the dark matter interaction cross-section with baryonic matter, so that a comparison with direct detection experiments is allowed.

Keywords: dark matter; LHC; HEP; ATLAS; CMS

1. Introduction

The existence of dark matter (DM) is well established in modern physics, due to several astronomical observations [1,2]. Precise measurements from the Planck experiment [3] estimate that DM composes 25% of the total Universe mass-energy budget; nevertheless, its nature is still unknown. Several searches for DM have been put in place in the last few decades, assuming it is made of particles that interact weakly with the known matter (weakly-interacting massive particles (WIMPs)). In this document, the main searches performed using the CMS [4] and ATLAS [5] detectors, exploiting data collected during the first part of Run 2 of the Large Hadron Collider (LHC) data taking are presented. The integrated luminosity collected by each experiment during this data-taking period is about 36 fb^{-1} .

2. Search for Dark Matter at the LHC

The LHC is a 27 km-long circular hadron accelerator and collider located in the underground tunnel originally built for the Large Electron Positron collider (LEP). It currently represents the best machine to search for new physics, thanks to two characteristics:

- The unprecedented collisions' center-of-mass energy (13 TeV during Run 2) allows it to be sensitive to the production of new heavy mediators.
- Thanks to the high instantaneous luminosity ($\mathcal{L} = 2 \times 10^{34} \text{ cm}^{-2} \text{ s}^{-1}$), also rare processes with cross-sections of the order of the fb can be inspected.

CMS and ATLAS, the two multipurpose detectors located along the LHC ring, at two of the beam interaction points, exploit similar analysis techniques in order to detect the presence of DM, which is not expected to interact in the detector:

- In mono-X searches, a dark matter mediator is produced by the annihilation of a pair of quarks or gluons and then decays to a pair of WIMPs, which escape the experimental device undetected. To trigger this kind of event, the presence of a detectable SM particle in the event is required. The fact that the WIMPs cannot be recorded creates an imbalance in the momentum measured in the transverse plane, called missing transverse energy (E_T^{miss}) or missing transverse momentum (p_T^{miss}), which is a key property of these searches.
- In mediator searches, the dark matter mediator decays to a pair of quarks or leptons, producing a localized excess of events in the invariant mass spectrum or in specifically chosen angular distributions.

A visual representation of the two approaches is shown in Figure 1.

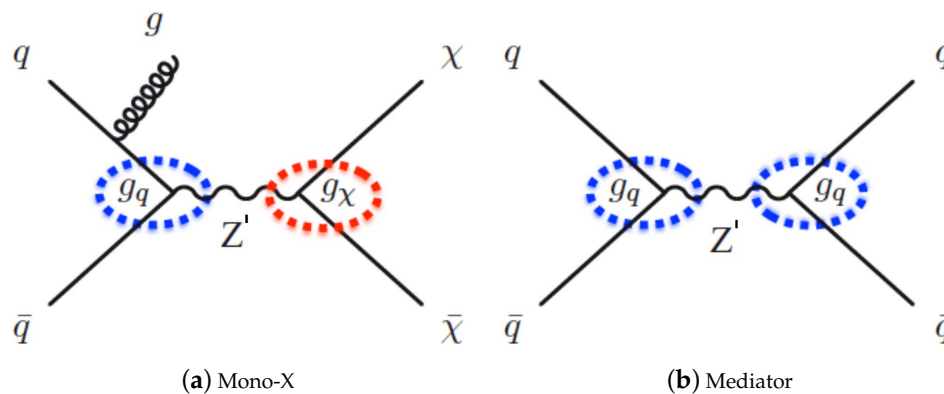


Figure 1. Schematic representation of the two search techniques presented in this document.

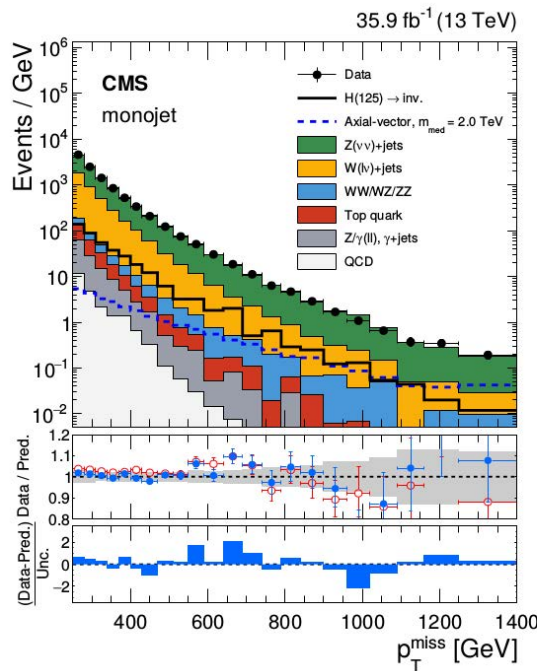
3. Mono-X Searches

Mono-X searches at CMS and ATLAS follow the recommendations of the ATLAS/CMS Dark Matter Forum [6] for the choice of the models to inspect and their parameters. Particular attention is dedicated to the nature of the mediator, which can be a scalar, a pseudo-scalar, a vector, or an axial-vector, and to the couplings with quarks, leptons, and dark matter particles. Typically, scans over the mediator and dark matter particle masses are performed, so that results are provided in terms of limits on the dark matter production cross-section, as a function of the mediator and dark matter particle mass, and given a certain set of couplings. Several final states with different SM particles have been inspected: in mono-jet, mono- γ and mono-Z searches, the SM particle is emitted as initial state radiation (ISR), while in mono-top, mono-Higgs, and $t\bar{t}$ + DM searches, different kinds of models are taken as references. In this section, the current mono-X analyses are described, giving basic details regarding the analysis strategy, the models inspected, and showing the main results.

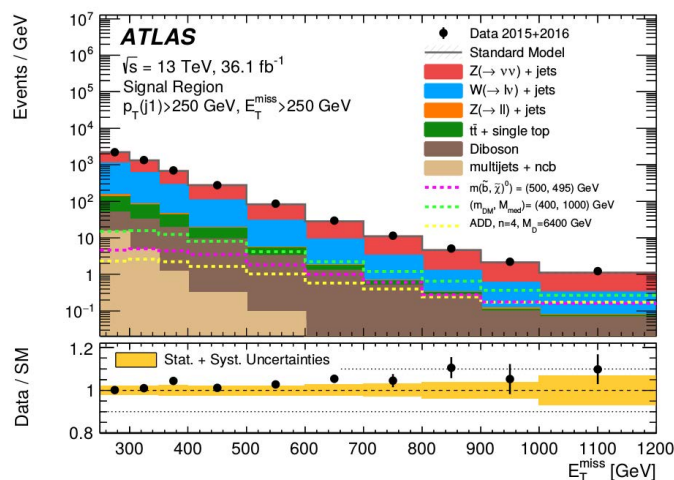
3.1. Mono-Jet

The mono-jet channel is currently the most sensitive mono-X search, due to the high probability of emitting an ISR jet. The analysis strategy is similar for CMS and ATLAS and consists of requiring one energetic jet recoiling against a large amount of E_T^{miss} . Both experiments select events with $p_T^{\text{miss}} > 250$ GeV, while the jet p_T thresholds are different: 100 GeV for CMS [7], and 250 GeV for ATLAS [8]. The leading jet and the p_T^{miss} are expected to be produced back-to-back, so that an angular separation in the transverse plane of 0.5 (0.4) radians is required by CMS (ATLAS). Events with additional leptons or photon are rejected. The main backgrounds are the represented by the production of $Z \rightarrow \nu\bar{\nu}$ + jets and $W \rightarrow \ell\nu$ + jets, which are estimated in dedicated control regions (CRs). The Z + jets process is estimated in a di-lepton control region, enriched in $Z \rightarrow \ell^+\ell^-$ events, in which the momenta of the leptons are used in the computation of the p_T^{miss} . In addition, CMS includes a γ + jets control region, in which the photon transverse energy is included in the E_T^{miss}

computation. Similarly, the $W + \text{jets}$ background is estimated in a single-lepton control region, where the lepton momentum is used in the p_T^{miss} computation. The signal extraction is performed through a simultaneous fit to the p_T^{miss} spectrum in the signal region and in the control regions and is interpreted in terms of vector or axial-vector mediators. In Figure 2, the expected and observed p_T^{miss} distributions in the signal regions for CMS and ATLAS are shown. In both cases, no significant discrepancies with respect to the SM predictions are observed, so that the results can be interpreted as limits on the DM mediator, and final state particle masses are set, as shown in Figure 3. Assuming a coupling of the DM mediator to quarks of 0.25 and a coupling of the mediator to the WIMP particles χ , mediators of masses up to 1.8 TeV and DM particles of masses up to 700 GeV are excluded.

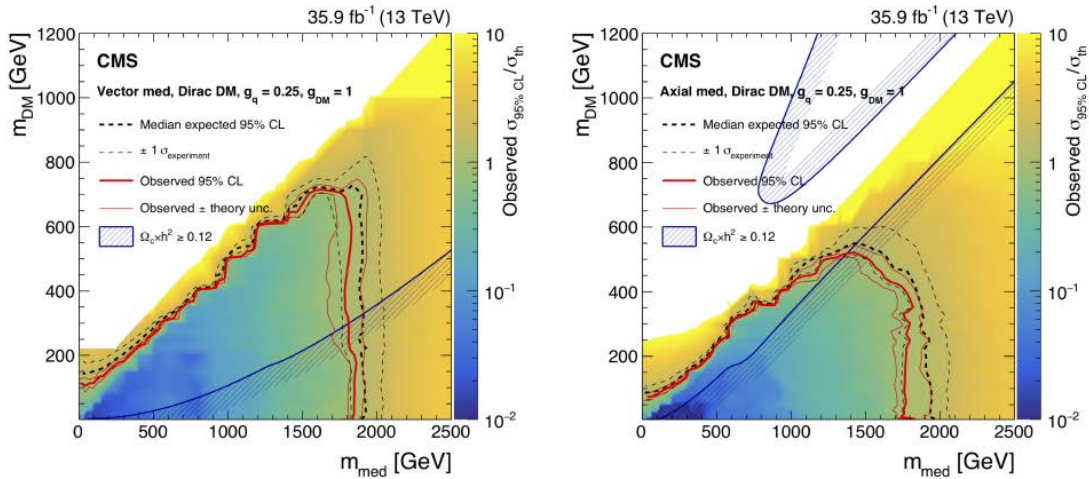


(a) CMS

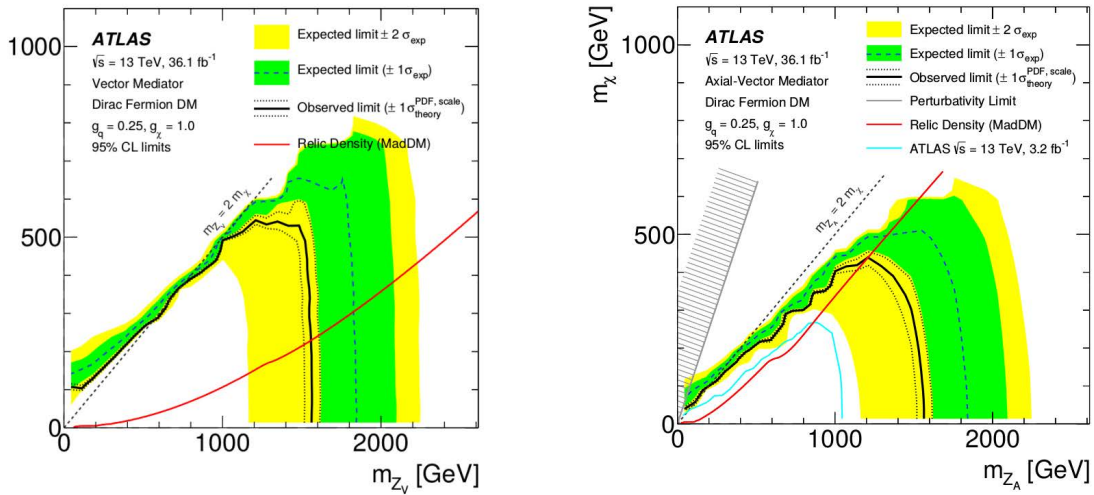


(b) ATLAS

Figure 2. Data-Montecarlo (MC) distributions of the mono-jet signal regions for the CMS [7] (a) and ATLAS [8] (b) analyses.



(a) CMS



(b) ATLAS

Figure 3. Exclusion limits for the CMS [7] (a) and ATLAS [8] (b) mono-jet analyses. On the left-side plots, results are interpreted in terms of the vector mediator, and on the right-side, plots in terms of the axial-vector mediator. In both cases, the DM particles are considered as Dirac fermions. The coupling of the mediator to quarks (g_q) is set to 0.25, and the coupling of the mediator to DM (g_{DM} or g_χ) is fixed to one.

3.2. Mono- γ

The mono- γ search is similar to the mono-jet one, with the difference that the probability to emit a photon from ISR is lower than the probability to emit a jet, so that the analysis is slightly less sensitive. Furthermore, in this case, the basic selection consists of requiring one energetic photon, with a transverse energy larger than 175 GeV (150 GeV) for CMS [9] (ATLAS [10]), and rejecting events with reconstructed leptons or jets. An additional selection of p_T^{miss} larger than 170 GeV is set by CMS, while ATLAS introduces the quantity $\frac{E_T^{\text{miss}}}{\sqrt{\sum E_T}}$, which must be larger than $8.5 \text{ GeV}^{1/2}$, and effectively rejects $\gamma + \text{jets}$ events. The main backgrounds are, similarly to the mono-jet case, the $Z \rightarrow \nu\bar{\nu} + \gamma$ and the $W \rightarrow \ell\nu + \gamma$ processes, but also the production of single electrons or jets reconstructed as photons. The contamination of the first two backgrounds is estimated in dedicated control regions with one (for $W \rightarrow \ell\nu + \gamma$) or two leptons (for $Z \rightarrow \nu\bar{\nu} + \gamma$). The estimation of the electron-induced background and the jet-induced background is performed by both experiments measuring the probability of

reconstructing an electron or a hadronic jet as a photon and then re-weighting events in $e+ E_T^{\text{miss}}$ or loosely-identified photons + E_T^{miss} regions. The results are obtained via a simultaneous fit to the signal and control regions and are illustrated in Figure 4. Also in this case, they are interpreted in terms of vector or axial-vector mediators and assuming the same couplings as in the mono-jet analysis. In the vector-mediator interpretation, mediator masses up to 1200 GeV, and DM particle masses up to 500 GeV are excluded. In the axial-vector interpretation, the same mediator masses are ruled out, while the exclusion of m_χ reaches 350 GeV.

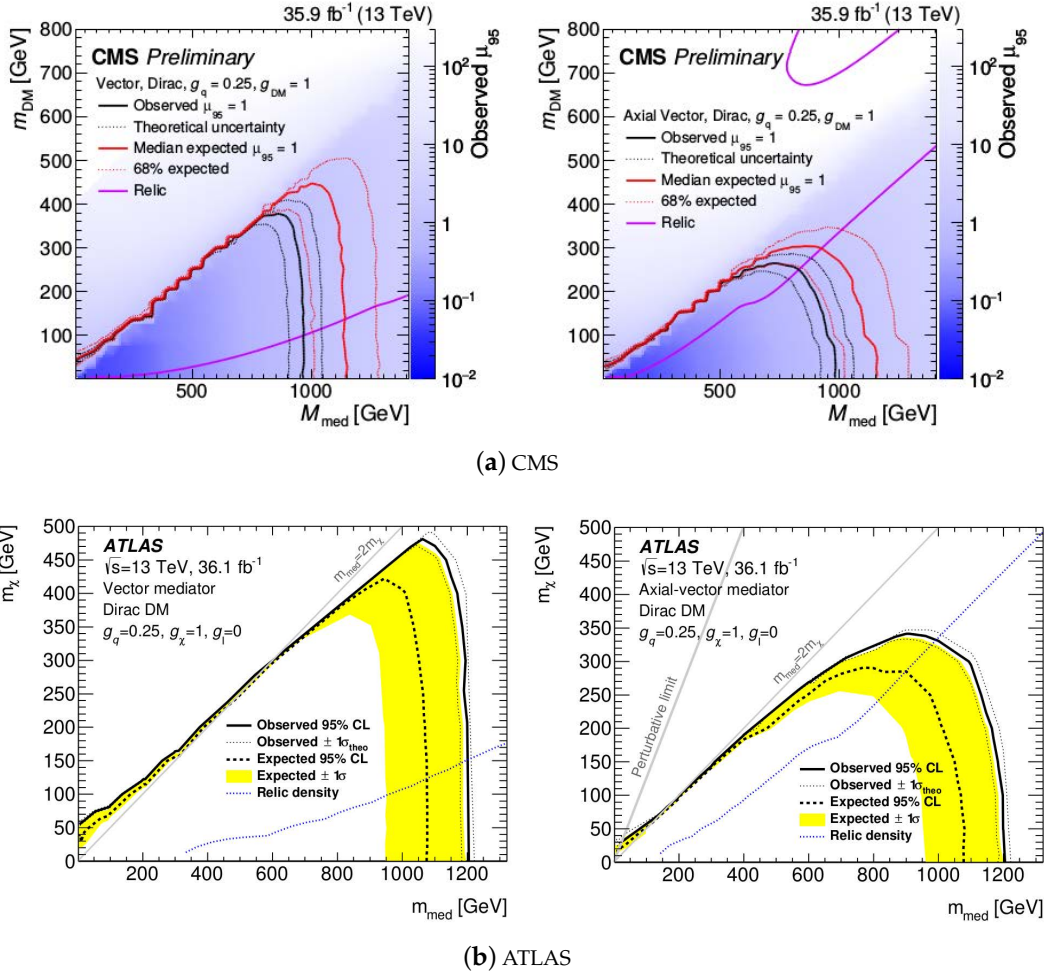


Figure 4. Exclusion limits for the CMS [9] (a) and ATLAS [10] (b) mono- γ analyses. On the left-side plots, results are interpreted in terms of the vector mediator, and on the right-side, plots in terms of the axial-vector mediator. In both cases, the DM particles are considered as Dirac fermions. The coupling of the mediator to quarks (g_q) is set to 0.25, and the coupling of the mediator to DM (g_{DM} or g_χ) is fixed to one.

3.3. Mono-Z

The mono-Z signature can be easily tagged by requiring events with two same-sign leptons with invariant mass compatible with m_Z and large E_T^{miss} (at least 100 GeV for CMS [11], or 90 GeV for ATLAS [12]). Additionally, events with more than two reconstructed leptons or with at least one reconstructed b-jet are rejected. The main backgrounds are represented by the $ZZ \rightarrow l^+ l^- \nu \bar{\nu}$ and $WZ \rightarrow l \nu l^+ l^-$ processes. The former is estimated by ATLAS directly using MC simulation, while in CMS, a control region with a tightly-identified same-sign lepton pair and a loosely-identified same-sign lepton pair, both compatible with the decay of a Z boson, is used to describe the E_T^{miss} of the process. Here, the loose lepton pair is included in the E_T^{miss} computation. For the latter, both experiments define

a control region with three leptons to estimate the contamination in the signal region. The results are extracted through a fit to the E_T^{miss} and are interpreted in terms of limits on the production of the vector and axial-vector mediator by CMS and in terms of the axial-vector mediator for ATLAS, as shown in Figure 5. The same couplings as in the mono-jet and mono- γ analyses are used in this search. The vector-mediator mediator of a mass up to 680 GeV and the DM particle of mass up to 250 GeV are excluded. In the axial-vector interpretation, mediator masses up to 700 GeV and m_χ up to 150 GeV are excluded.

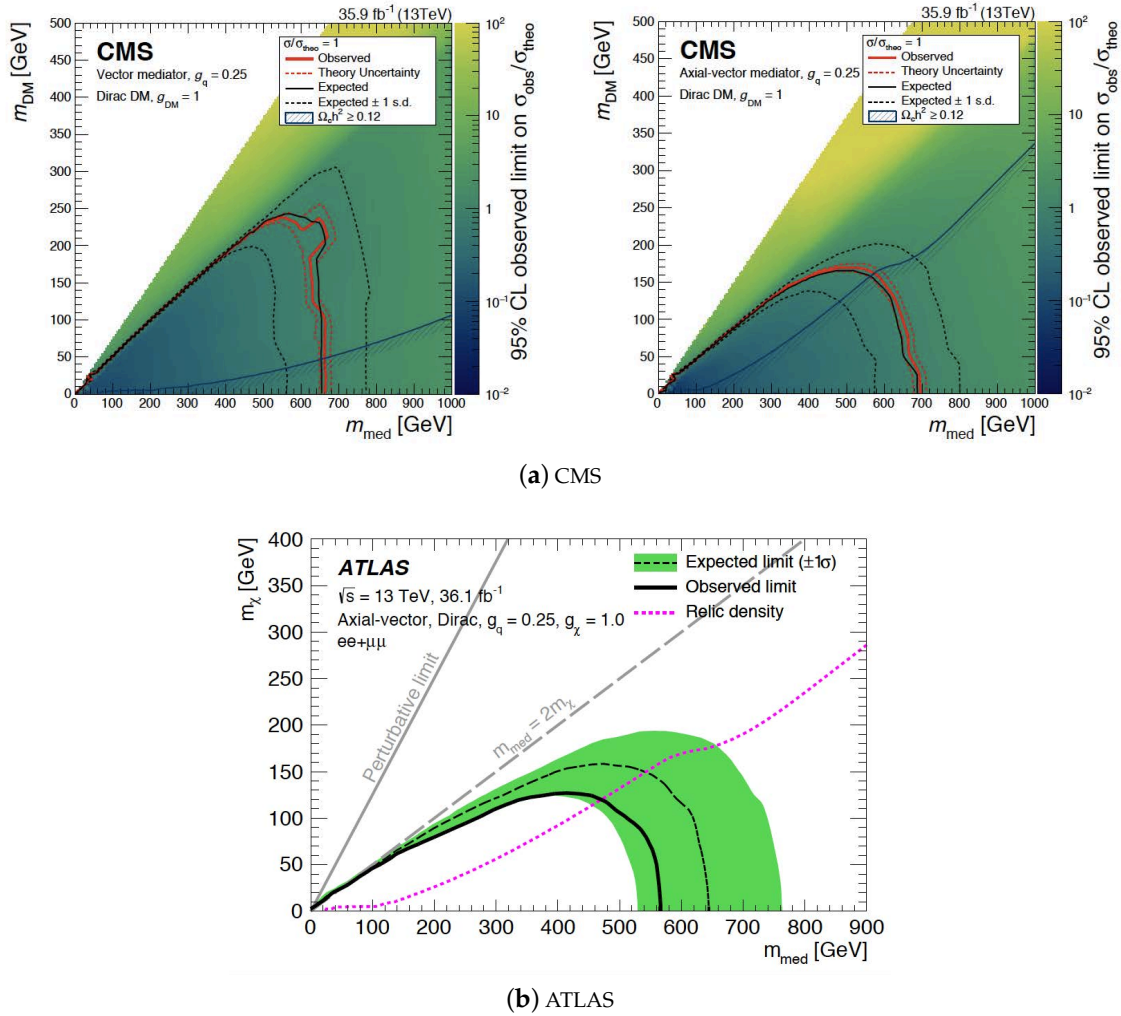
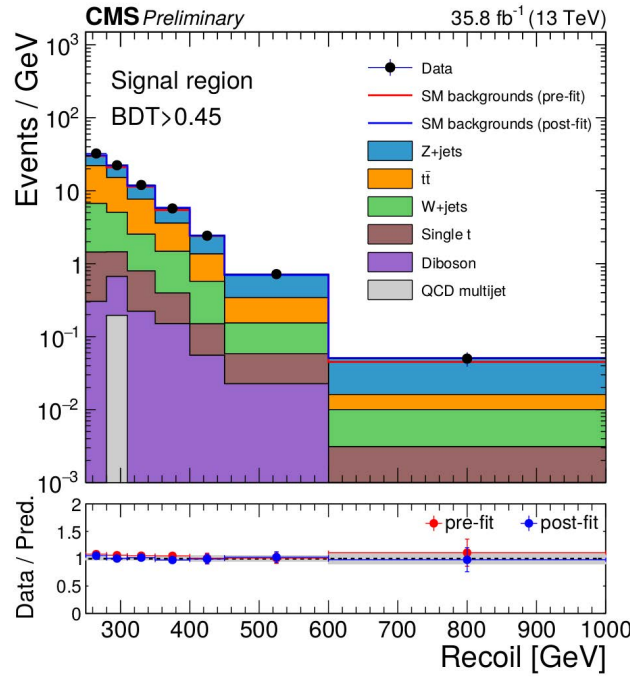


Figure 5. Exclusion limits for the CMS [11] (a) and ATLAS [12] (b) mono-Z analyses. CMS interpreted the results in terms of the vector mediator (a-left) and the axial-vector mediator (a-right), while ATLAS provided interpretation only for the axial-vector mediator. In both cases, the DM particles are considered as Dirac fermions. The coupling of the mediator to quarks (g_q) is set to 0.25, and the coupling of the mediator to DM (g_{DM} or g_χ) is fixed to one.

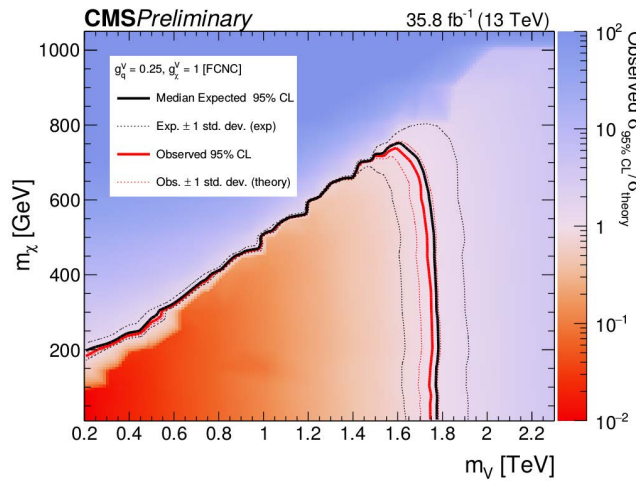
3.4. Mono-Top

The search for mono-top has been carried out only by the CMS collaboration [13]. The model inspected differs from the previous ones, since a flavor-changing neutral current (FCNC) is introduced in this case. The analysis selects events with an energetic jet ($p_T > 250$ GeV) with a mass compatible with a top quark and tagged as produced by a top quark by a dedicated set of boosted decision trees (BDT). The jet has to recoil against a large amount of E_T^{miss} (at least 250 GeV). Several control regions are defined to estimate the background contamination in the signal region using data. The main background, $Z \rightarrow \nu\bar{\nu} + \text{jets}$, is estimated using a di-electron, a di-muon, and a $\gamma + \text{jets}$ control region,

where the momenta of the muons, or of the electrons, or the transverse energy of the photon are included in the E_T^{miss} computation. Secondary backgrounds, $W \rightarrow \ell\nu + \text{jets}$ and semi-leptonic $t\bar{t}$ decays, are estimated in single lepton control regions, which can include a b-jet (top CR) or require b-veto ($W + \text{jets}$ CR). The results are extracted through a simultaneous fit to the signal region and the control region, on the E_T^{miss} , and are interpreted as limits on the mass of the flavor-changing vector boson and on the DM particle mass (see Figure 6). In particular, the exclusion reaches 1.8 TeV for the mediator mass and 750 GeV for the DM particle mass, fixing the coupling of the mediator to quarks to 0.25, and the coupling to DM particles to one.



(a) E_T^{miss} spectrum



(b) Limits

Figure 6. E_T^{miss} distribution in the mono-top [13] signal region (a), and limits on the mass of the vector boson (flavor-changing neutral current (FCNC)) versus the mass of the DM particle (b). The coupling of the vector boson to quarks (g_q^V) is set to 0.25 and the coupling to DM (g_χ^V) to one.

3.5. Mono-Higgs

The emission of a Higgs boson from ISR is strongly suppressed, due to the low coupling with light quarks and due to the loop-mediated interaction with massless gluons. This implies that models typically inspected in mono- X searches are not valid in the mono-Higgs case. Instead, a Z' -2HDM model and a Z' -Baryonic model, shown in Figure 7, are studied. Here, the Higgs boson directly interacts with the mediator, so that Higgs-mediator coupling is accessible with these models. Different Higgs decay channels are inspected by CMS ($h \rightarrow b\bar{b}$ [14,15], and a combination of $h \rightarrow \gamma\gamma$ and $h \rightarrow \tau\tau$ [16]) and ATLAS ($h \rightarrow b\bar{b}$ [17] and $h \rightarrow \gamma\gamma$ [18]).

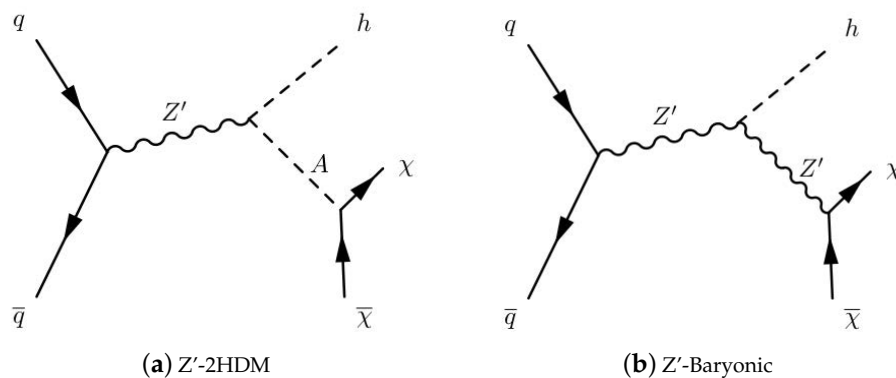
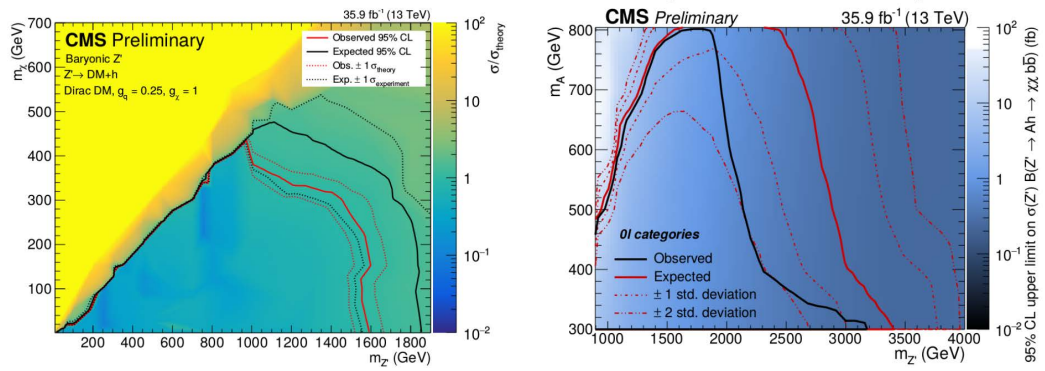


Figure 7. Simplified models inspected by mono-Higgs analyses. On the (a), the Z' -2HDM model, and on the (b), the Z' -baryonic model.

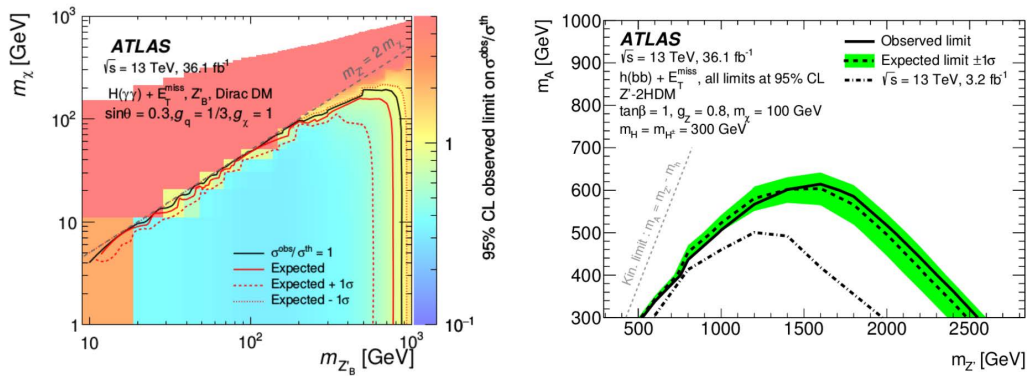
The analysis strategy is similar in all cases: tag the Higgs boson through invariant mass requirements, and require it to recoil against a significant amount of E_T^{miss} . The main backgrounds are estimated using data in the invariant mass side-bands or in specific control regions, and the results are extracted through a fit to significant variables, as the invariant mass, the E_T^{miss} , or the transverse mass, defined as:

$$m_T = \sqrt{2 \cdot p_T^{\ell\ell} \cdot E_T^{\text{miss}} \cdot (1 - \cos \Delta\phi(\ell\ell, E_T^{\text{miss}}))} \quad (1)$$

The most significant interpretations of the results, from CMS and ATLAS, and for the two models are shown in Figure 8. For the Z' -baryonic model, assuming the coupling between the mediator and quarks to be 0.25 and the coupling of the mediator to DM particles to be one, a Z' mediator lighter than 1.6 TeV and DM particles lighter than 450 GeV are excluded. For the Z' -2HDM model, the Z' coupling strength is 0.8, and the mass of the DM particles is fixed to 100 GeV. With these parameters, Z' masses up to 3.2 TeV and DM masses up to 800 GeV are excluded.



(a) CMS

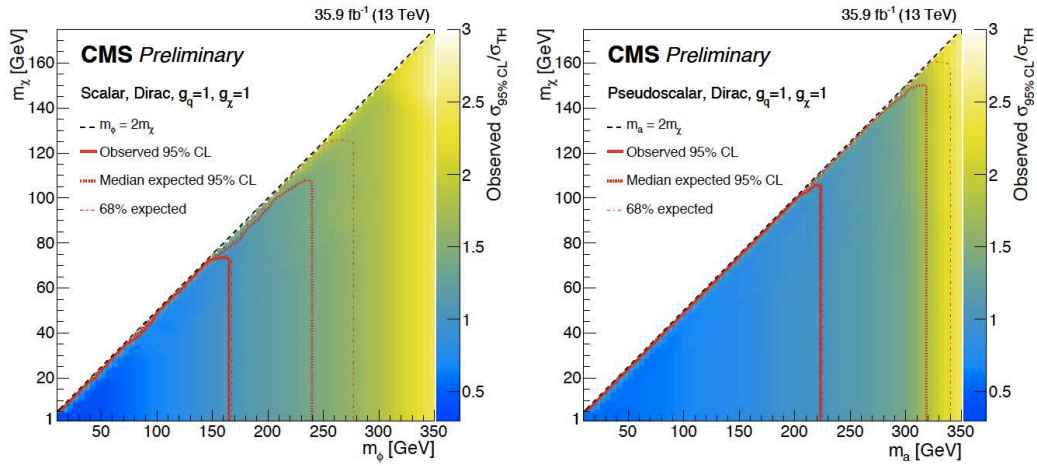


(b) ATLAS

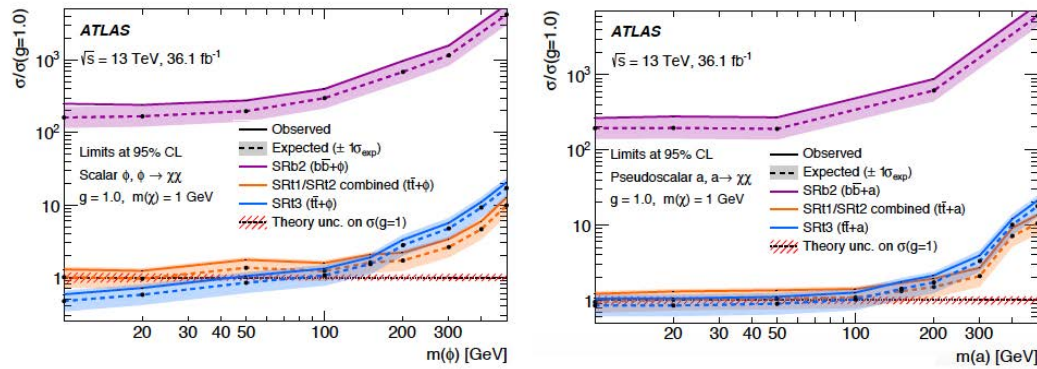
Figure 8. Main results for the mono-Higgs analyses in CMS [14,15] (a) and ATLAS [17,18] (b). On the left, the Z'-baryonic interpretation is shown, and on the right, the Z'-2HDM.

3.6. $t\bar{t}$ + Dark Matter

The production of dark matter in association with a pair of top quarks is favored in models in which Yukawa coupling between the mediator and SM particles is expected, due to the large mass of the top. The three possible final states, with 0, 1 or 2 leptons, are inspected, and CMS combined the results together [19], while ATLAS did not perform a full combination [20,21]. Depending on the final state, events with top quarks are selected by requiring the presence of b-tagged (zero or one lepton) or top-tagged jets (fully hadronic final state). Additionally, events must present a large amount of E_T^{miss} . Different definitions of the transverse mass of the event, depending on the number of leptons in the final state, are used to discriminate the signal from the dominant $t\bar{t}$ background. The presence of undetectable DM particles tends in fact to produce m_T distributions with larger tails in the signal, with respect to the background. The results are obtained through a fit to the E_T^{miss} variable and are shown in Figure 9, both for CMS and ATLAS. In the case of the scalar mediator interpretation, mediator masses up to 165 GeV and DM particle masses up to 75 GeV are excluded, while in the case of the pseudoscalar mediator, mediators with masses up to 225 GeV and DM particles of masses up to 105 GeV are ruled out.



(a) CMS



(b) ATLAS

Figure 9. Main results for the $t\bar{t}$ + DM analyses in CMS [19] (a) and ATLAS [21] (b). On the left, the results for a scalar mediator are shown, and on the right, the results for a pseudoscalar mediator. Both the coupling of the mediator to quarks (g_q) and the coupling to DM (g_χ) are set to one. CMS presented the results of the combination of three $t\bar{t}$ final states as limits on the mediator mass versus DM particle mass. ATLAS fixed the m_χ to 1 GeV and showed the limits on the mediator mass, without combining the results of the different final states.

4. Mediator Searches

Assuming that a DM mediator can be produced by quark-quark annihilation implies that it can also decay to a pair of quarks. Mediator searches focus on final states with two jets, typically looking for a bump in the di-jet invariant mass spectrum, due to the presence of a new resonance. The di-jet production at the LHC is very abundant, so that these searches are usually able to inspect high mass ranges and put stringent limits. On the other hand, due to the very high rate of production, particularly of pairs of low- p_T jets, traditional di-jet searches are not sensitive to low-mass mediators, since typically, high jet- p_T thresholds have to be set to avoid the saturation of the trigger bandwidth. Trigger-level analysis, making use of events with a limited amount of information, and searches for boosted mediators recoiling against hard ISR jets have been implemented to increase the sensitivity to lighter mediators. Finally, to search for broad resonances, which would be impossible to distinguish from the SM quantum chromodynamics (QCD) m_{jj} falling spectrum, analyses based on di-jet angular distribution have been designed: SM jet pairs are usually produced in the forward region of the detector, while heavy mediators would preferentially emit jets in the barrel. Since these searches involve only the coupling between mediator and quarks, they can be used to put constraints on this parameter or, fixing the coupling value, to put upper limits on the mediator mass.

4.1. Di-Jet Searches

The standard mediator-search approach consists of selecting events with two reconstructed jets in the final state and plotting their invariant mass. The distribution is fitted with a smooth function, since QCD predicts a smoothly-falling m_{jj} spectrum, looking for excesses or deviations in data with respect to the fit results, as shown in Figure 10. Due to the abundant QCD production of events with jet pairs at the LHC, to avoid the saturation of the trigger bandwidth, events with very energetic jets can be selected. For this reason, this kind of analysis is sensitive to very high mass mediators, with masses larger than 1.6 TeV for CMS [22] and 1.5 TeV for ATLAS [23].

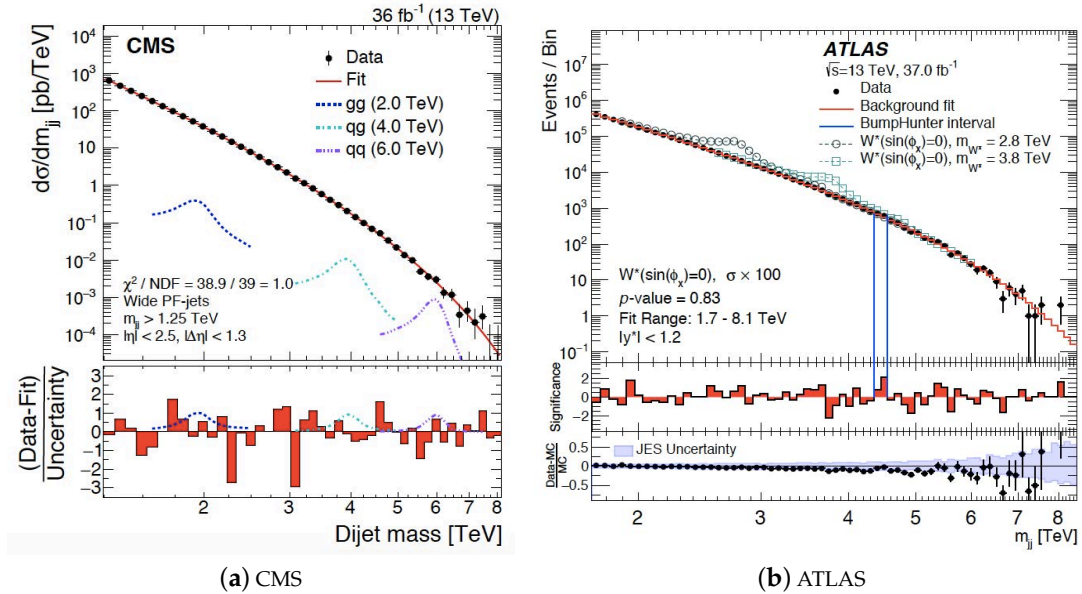


Figure 10. Di-jet invariant mass distributions for the CMS [22] (a) and the ATLAS [23] (b) analyses.

The results are interpreted as upper limits on the quark-mediator coupling, as a function of the mediator mass, and are displayed in Figure 11. The most stringent limit is given by ATLAS, for $m_{med} = 1.5$ TeV, and corresponds to $g_q = 0.08$.

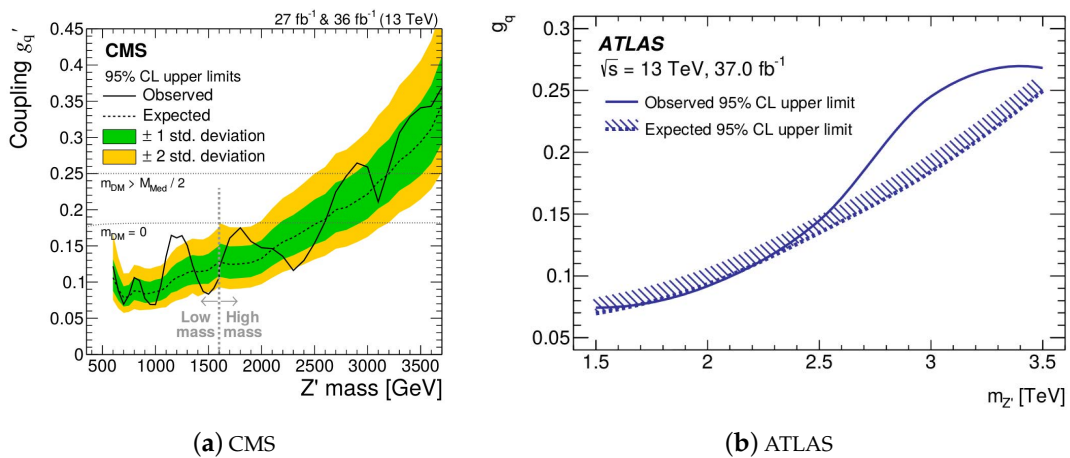


Figure 11. Results for the CMS [22] (a) and the ATLAS [23] (b) mediator searches. Limits on the mediator coupling to quarks (g_q) as a function of the mediator mass are set. The CMS plot shows also the results for low-mass mediator searches, for $m_{med} < 1.6$ TeV.

4.2. Low-Mass Di-Jet Searches

The main limiting factor in the search for low-mass mediators in the finite trigger bandwidth of the CMS and ATLAS experiments. In order to avoid this inconvenience, two techniques have been exploited in dedicated analyses:

- Save only limited relevant information at the trigger level to enhance the rate of data acquisition. This means that events can be reconstructed faster, and occupy less space, allowing one to lower the jet p_T thresholds, hence being sensitive to lighter mediators. In particular, ATLAS [24] managed to push the sensitivity down to resonances of 450 GeV and CMS [25] to 500 GeV.
- Select events in which the two jets are highly boosted and merged together, due to recoil against an additional hard ISR jet. This means that even for very light resonances, the event presents potentially three high- p_T jets able to pass the standard trigger thresholds. This analysis has been performed by CMS [26] and is sensitive to di-jet invariant masses between 50 GeV and 300 GeV.

The results of these low-mass di-jet analyses are shown in Figure 11 (low-mass region in the left plot for CMS) and in Figure 12. They are interpreted as limits on the coupling between quarks and the DM mediator: couplings lower than 0.03 are excluded for $m_{\text{med}} = 800$ GeV by ATLAS, and couplings lower than 0.06 are excluded for $m_{\text{med}} = 60$ GeV by CMS.

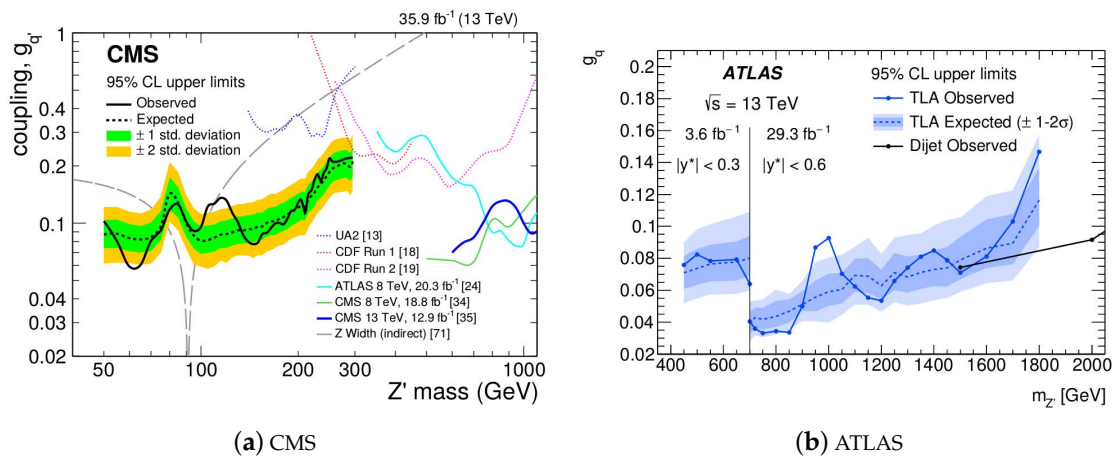


Figure 12. Results for the CMS [26] (a) and the ATLAS [24] (b) low-mass mediator searches. Limits on the mediator coupling to quarks (g_q) as a function of the mediator mass are set. The CMS plot shows the results for the initial state radiation (ISR)-low-mass mediator search, while the ATLAS results refer to the trigger-level analysis.

4.3. Di-Jet χ Searches

In the case of broad resonances, the classic bump search may not be the optimal analysis strategy, since it would be difficult to distinguish the peak of resonant events over the falling QCD spectrum. On the other hand, the jet angular distribution is not sensitive to the resonance width, but is a good variable to discriminate signal and background. In particular, it is common to define χ as:

$$\chi = e^{y_1 - y_2} = \frac{1 + \cos \theta^*}{1 - \cos \theta^*} \quad (2)$$

where y_1 and y_2 are the rapidities of the jets and θ^* is the polar angle in the center-of-mass system. The definition has been chosen since QCD events are expected to present angular distributions independent of χ , while heavy mediators would preferentially produce events with low values of χ . The results are interpreted in different frameworks by the CMS [25] and ATLAS [23] collaborations. In CMS, limits are set on the mass of the mediator, assuming the coupling with quarks equal to one:

resonance masses between 2 TeV and 4.6 TeV are ruled out. The ATLAS interpreted as limits on the energy scale Λ of contact interactions: considering constructive (destructive) interference with QCD, values of Λ smaller than 21 TeV (13 TeV) are excluded. The results are presented in Figure 13.

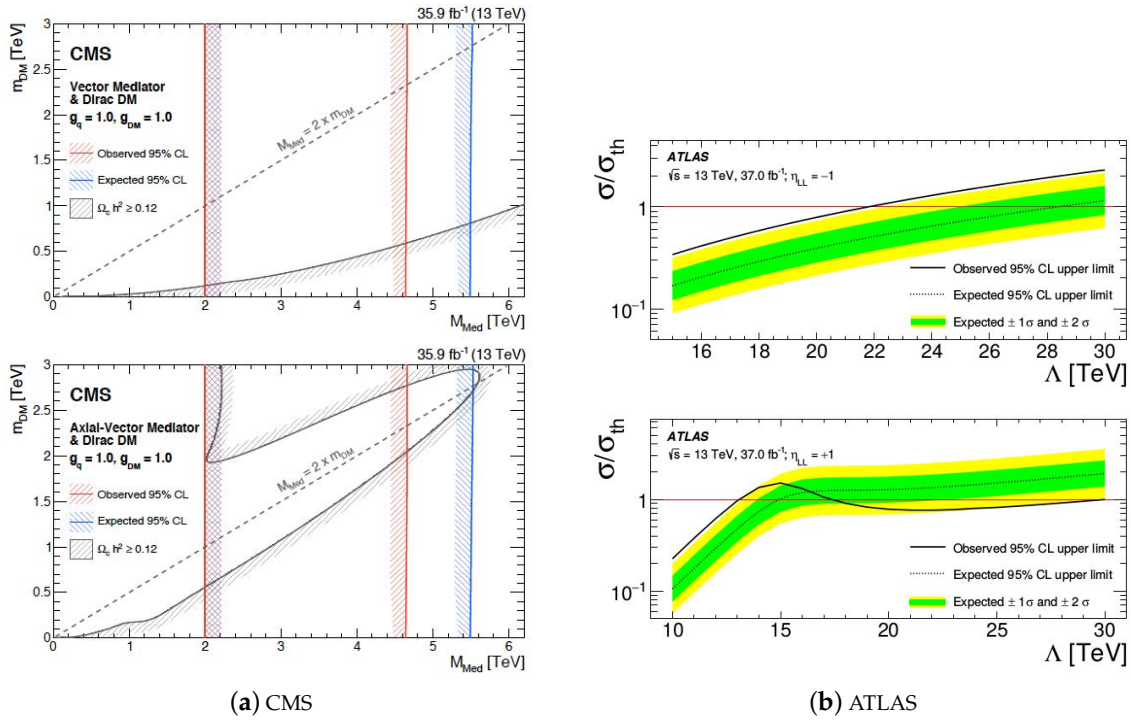
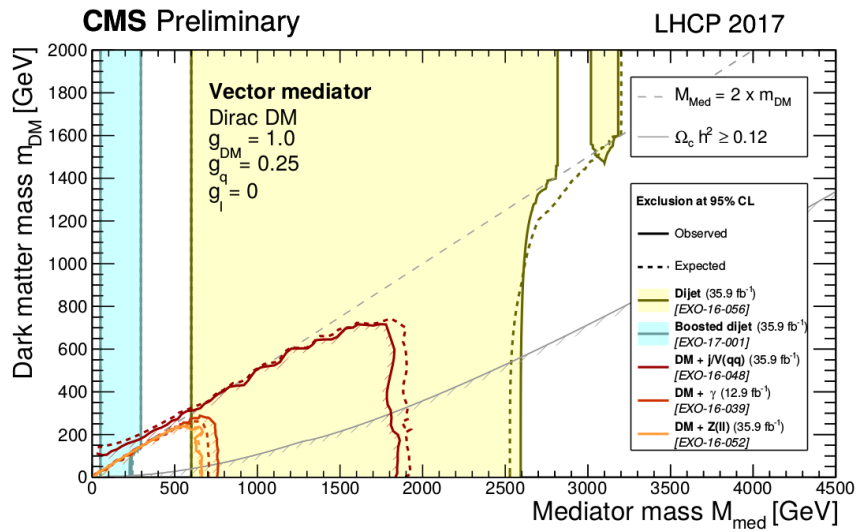


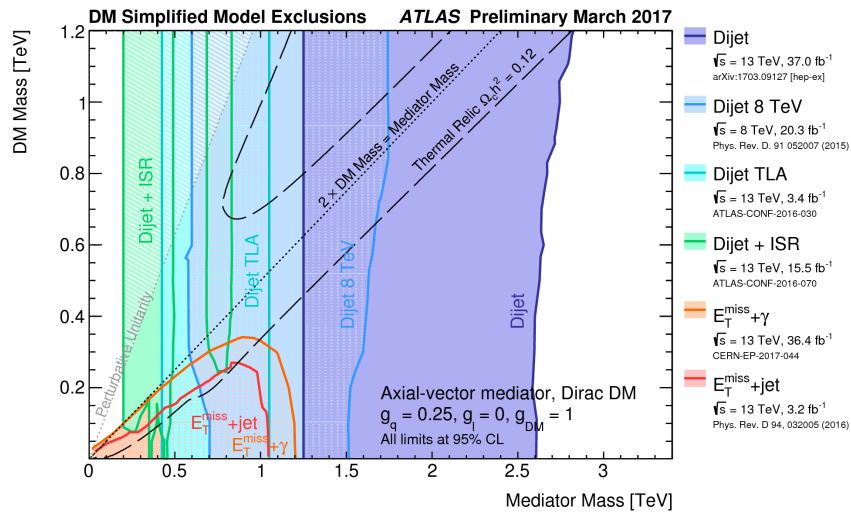
Figure 13. Results for the CMS [25] (a) and the ATLAS [23] (b) di-jet χ searches. CMS results assume a coupling g_q between quarks and mediator of one, while ATLAS considers effective interactions characterized by a single energy scale Λ .

5. Comparison of Results and Reinterpretation

The results of all the searches can be compared by fixing the mediator couplings and plotting the corresponding exclusion limits in terms of masses of the mediator versus masses of DM particles, which are ruled out. Summary plots for CMS [27] and ATLAS [28] are presented in Figure 14, assuming coupling of the mediator to DM (g_{DM}) to one, to quarks (g_q) to 0.25, and to leptons (g_l) to zero. The CMS results presented in this document show the vector mediator interpretation, and the ATLAS results show the axial-vector mediator interpretation. The exclusion limits are dominated by the di-jet analyses, which profit from the large di-jet production cross-section and do not depend on the mass of the DM particles, which are not directly involved in this kind of search. The strong dependence of the results on the particular choice of the couplings is shown in Figure 15, where the same exclusion plots are displayed, but introducing a coupling of the mediator with leptons and reducing the coupling to quarks. In this case, stringent limits from di-lepton searches significantly reduce the phase space excluded by mono-X or mediator analyses.

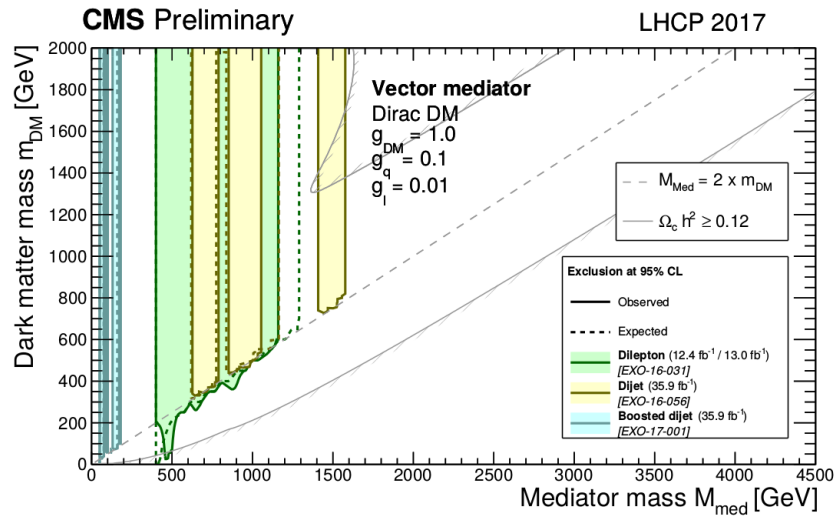


(a) CMS

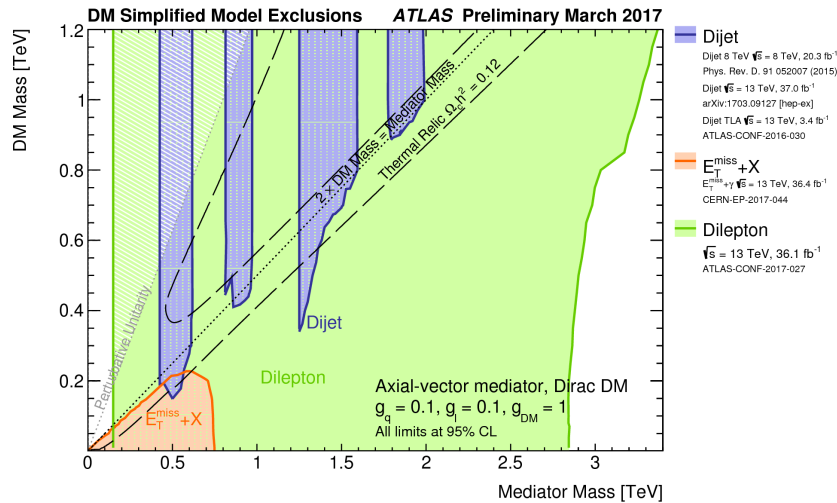


(b) ATLAS

Figure 14. Summary plots for the CMS [27] (a) and ATLAS [28] (b) dark matter searches. The coupling of the mediator to DM (g_{DM}) is set to one, to quarks (g_q) to 0.25, and to leptons (g_l) to zero. The CMS results refer to the vector-mediator interpretation and the the ATLAS results to the axial-vector mediator.



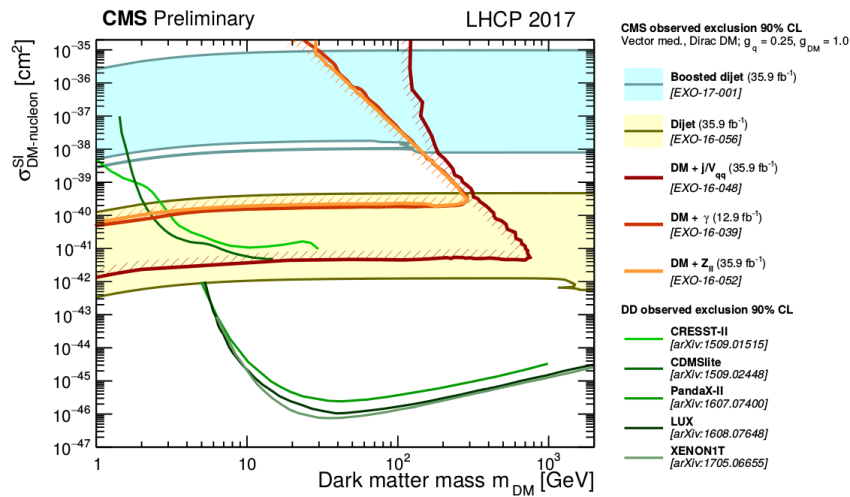
(a) CMS



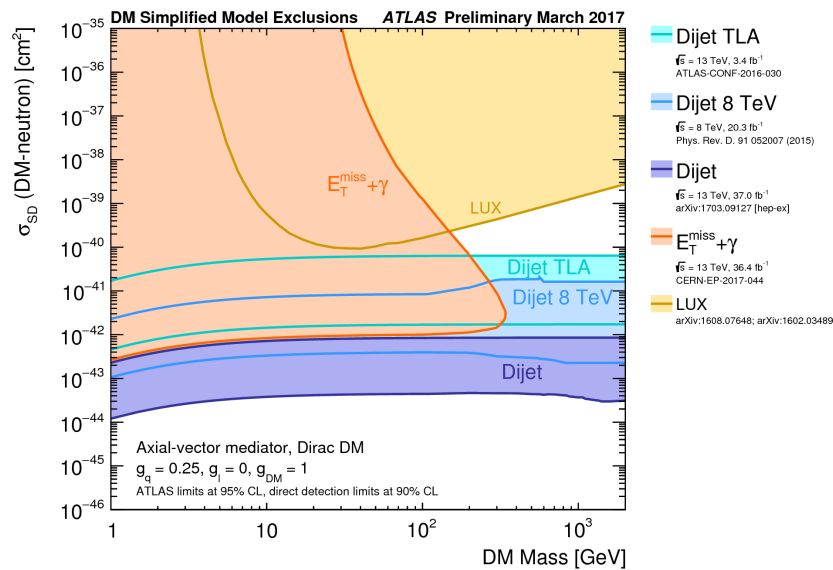
(b) ATLAS

Figure 15. Summary plots for the CMS [27] (a) and ATLAS [28] (b) dark matter searches. The coupling of the mediator to DM (g_{DM}) is set to one, to quarks (g_q) to 0.1, and to leptons (g_l) to 0.1 (0.01 for CMS). The CMS results refer to the vector-mediator interpretation and the ATLAS results to the axial-vector mediator.

The results can be also reinterpreted in terms of the DM-nuclei scattering cross-section [29], to be compared with the results of direct-detection DM experiments. Axial-vector results can be interpreted as limits on spin-dependent scattering cross-sections, while results of vector mediator searches are reinterpreted as limits on spin-independent scattering cross-sections. The choice of the couplings strongly affects the comparison shown in Figure 16, where the same couplings as in Figure 14 are selected. Under this assumption, collider searches are show to be particularly effective at inspecting light dark matter particles, with masses of the order of 10 GeV or lower.



(a) CMS



(b) ATLAS

Figure 16. Summary of the reinterpretation of dark matter searches as the DM-nuclei scattering cross-section, for CMS [27] (a) and ATLAS [28] (b). The coupling of the mediator to DM (g_{DM}) is set to one, to quarks (g_q) to 0.25, and to leptons (g_l) to zero. The CMS results refer to spin-independent (vector-mediator) scattering and the the ATLAS results to the spin-dependent (axial-vector) interaction. The results from some of the main direct-detection and indirect-detection searches are also shown for comparison.

6. Conclusions

The main searches for dark matter performed by the CMS and ATLAS collaborations have been presented. Making use of data collected during 2016 with proton-proton collisions with a center-of-mass energy of 13 TeV by the LHC, for a total integrated luminosity of 36 fb^{-1} for each experiment, no significant discrepancies with respect to SM predictions have been found, so that the results have been interpreted as limits on the couplings of dark matter mediators to SM particles or as limits on the masses of the mediator and the DM particles. A further interpretation of the results as limits on the DM-nuclei scattering cross-section has been provided, in order to allow a comparison with results from experiments of the direct-detection of dark matter. This comparison strongly depends on the choice of the couplings between DM and SM particles and shows that collider searches are competitive in particular for low DM particles masses. Several searches are still limited by the low number of expected signal events, in particular mono-X searches, so that the sensitivity of the analyses will profit from the luminosity of the full Run 2 LHC data taking, which will include data collected between 2015 and 2018, for a total luminosity of more than 100 fb^{-1} .

Author Contributions: The research works presented in this report have been produced by several members of the ATLAS and CMS collaborations. The author collected the information and the public results, and summarized them in a single document.

Funding: This research was funded by Spanish FPI grant number BES-2015-071291, associated to project FPA2014-55295-C3-1-R.

Conflicts of Interest: The author declares no conflict of interest.

References

1. Roberts, M.S.; Rots, A.H. Comparison of Rotation Curves of Different Galaxy Types. *Astron. Astrophys.* **1973**, *26*, 483–485.
2. Clowe, D.; Bradac, M.; Gonzalez, A.H.; Markevitch, M.; Randall, S.W.; Jones, C.; Zaritsky, D. A direct empirical proof of the existence of dark matter. *Astrophys. J.* **2006**, *648*, L109–L113, doi:10.1086/508162. [[CrossRef](#)]
3. Ade, P.A.R.; Aghanim, N.; Arnaud, M.; Ashdown, M.; Aumont, J.; Baccigalupi, C.; Banday, A.J.; Barreiro, R.B.; Bartlett, J.G.; Bartolo, N.; et al. Planck 2015 results. XIII. Cosmological parameters. *Astron. Astrophys.* **2016**, *594*, A13, doi:10.1051/0004-6361/201525830. [[CrossRef](#)]
4. Chatrchyan, S.; Antchev, G.; Aspell, P.; Avati, V.; Bagliesi, M.G.; Berardi, V.; Berretti, M.; Boccone, V.; Bottigli, U.; Bozzo, M.; et al. The CMS Experiment at the CERN LHC. *J. Instrum.* **2008**, *3*, S08004, doi:10.1088/1748-0221/3/08/S08004. [[CrossRef](#)]
5. Aad, G.; Butterworth, J.M.; Thion, J.; Bratzler, U.; Ratoff, P.N.; Nickerson, R.B.; Seixas, J.M.; Grabowska-Bold, I.; Meisel, F. The ATLAS Experiment at the CERN Large Hadron Collider. *Jinst* **2008**, *3*, S08003, doi:10.1088/1748-0221/3/08/S08003. [[CrossRef](#)]
6. Abercrombie, D.; Akchurin, N.; Akilli, E.; Maestre, J.A.; Allen, B.; Gonzalez, B.A.; Andrea, J.; Arbey, A.; Azuelos, G.; Azzi, P.; et al. Dark Matter Benchmark Models for Early LHC Run-2 Searches: Report of the ATLAS/CMS Dark Matter Forum. *arXiv* **2015**, arXiv:hep-ph/1507.00966.
7. Sirunyan, A.M.; Tumasyan, A.; Adam, W.; Ambrogio, F.; Asilar, E.; Bergauer, T.; Brandstetter, J.; Brondolin, E.; Dragicevic, M.; Erö, J.; et al. Search for new physics in final states with an energetic jet or a hadronically decaying W or Z boson and transverse momentum imbalance at $\sqrt{s} = 13 \text{ TeV}$. *Phys. Rev. D* **2018**, *D97*, 092005, doi:10.1103/PhysRevD.97.092005. [[CrossRef](#)]
8. Aaboud, M.; Aad, G.; Abbott, B.; Abdinov, O.; Abeloos, B.; Abidi, S.H.; AbouZeid, O.S.; Abraham, N.L.; Abramowicz, H.; Abreu, H.; et al. Search for dark matter and other new phenomena in events with an energetic jet and large missing transverse momentum using the ATLAS detector. *J. High Energy Phys.* **2018**, *1*, 126, doi:10.1007/JHEP01(2018)126. [[CrossRef](#)]
9. Sirunyan, A.M.; Tumasyan, A.; Adam, W.; Asilar, E.; Bergauer, T.; Brandstetter, J.; Brondolin, E.; Dragicevic, M.; Erö, J.; Flechl, M.; et al. Search for new physics in the monophoton final state in proton-proton collisions at $\sqrt{s} = 13 \text{ TeV}$. *J. High Energy Phys.* **2017**, *10*, 73, doi:10.1007/JHEP10(2017)073. [[CrossRef](#)]

10. Aaboud, M.; Åkerstedt, H.; Bendtz, K.; Bertoli, G.; Bessidskaia Bylund, O.; Bohm, C.; Carney, R.; Clément, C.; Cribbs, W.A.; Gellerstedt, K.; et al. Search for dark matter at $\sqrt{s} = 13$ TeV in final states containing an energetic photon and large missing transverse momentum with the ATLAS detector. *Eur. Phys. J.* **2017**, *C77*, 393, doi:10.1140/epjc/s10052-017-4965-8. [[CrossRef](#)] [[PubMed](#)]
11. Sirunyan, A.M. CMS Collaboration. Search for new physics in events with a leptonically decaying Z boson and a large transverse momentum imbalance in proton–proton collisions at $\sqrt{s} = 13$ TeV. *Eur. Phys. J.* **2018**, *C78*, 291, doi:10.1140/epjc/s10052-018-5740-1. [[CrossRef](#)]
12. Aaboud, M.; Aad, G.; Abbott, B.; Abdinov, O.; Abeloos, B.; Abidi, S.H.; AbouZeid, O.S.; Abraham, N.L.; Abramowicz, H.; Abreu, H.; et al. Search for an invisibly decaying Higgs boson or dark matter candidates produced in association with a Z boson in pp collisions at $\sqrt{s} = 13$ TeV with the ATLAS detector. *Phys. Lett.* **2018**, *B776*, 318–337, doi:10.1016/j.physletb.2017.11.049. [[CrossRef](#)]
13. *Search for Dark Matter in Final States with a Top Quark and Missing Transverse Momentum Using New Hadronic Top Quark Tagging Techniques*; Technical Report CMS-PAS-EXO-16-051; CERN: Geneva, Switzerland, 2017.
14. *Search for a Heavy Resonance Decaying into a Vector Boson and a Higgs Boson in Semileptonic Final States at $\sqrt{s} = 13$ TeV*; Technical Report CMS-PAS-B2G-17-004; CERN: Geneva, Switzerland, 2018.
15. *Search for Associated Production of Dark Matter with a Higgs Boson That Decays to a Pair of Bottom Quarks*; Technical Report CMS-PAS-EXO-16-050; CERN: Geneva, Switzerland, 2018.
16. *Search for Dark Matter Produced in Association with a Higgs Boson Decaying to $\gamma\gamma$ or $\tau^+\tau^-$ at $\sqrt{s} = 13$ TeV with the CMS Detector*; Technical Report CMS-PAS-EXO-16-055; CERN: Geneva, Switzerland, 2018.
17. Aaboud, M.; Aad, G.; Abbott, B.; Abdinov, O.; Abeloos, B.; Abidi, S.H.; AbouZeid, O.S.; Abraham, N.L.; Abramowicz, H.; Abreu, H.; et al. Search for Dark Matter Produced in Association with a Higgs Boson Decaying to $b\bar{b}$ using 36 fb^{-1} of pp collisions at $\sqrt{s} = 13$ TeV with the ATLAS Detector. *Phys. Rev. Lett.* **2017**, *119*, 181804, doi:10.1103/PhysRevLett.119.181804. [[CrossRef](#)] [[PubMed](#)]
18. Aaboud, M.; Aad, G.; Abbott, B.; Abdinov, O.; Abeloos, B.; Abidi, S.H.; AbouZeid, O.S.; Abraham, N.L.; Abramowicz, H.; Abreu, H.; et al. Search for dark matter in association with a Higgs boson decaying to two photons at $\sqrt{s} = 13$ TeV with the ATLAS detector. *Phys. Rev.* **2017**, *D96*, 112004, doi:10.1103/PhysRevD.96.112004. [[CrossRef](#)]
19. *Search for Dark Matter Produced in Association with a Top Quark Pair at $\sqrt{s} = 13$ TeV*; Technical Report CMS-PAS-EXO-16-049; CERN: Geneva, Switzerland, 2018.
20. Aaboud, M.; Aad, G.; Abbott, B.; Abdinov, O.; Abeloos, B.; Abidi, S.H.; AbouZeid, O.S.; Abraham, N.L.; Abramowicz, H.; Abreu, H.; et al. Search for top-squark pair production in final states with one lepton, jets, and missing transverse momentum using 36 fb^{-1} of $\sqrt{s}=13$ TeV pp collision. *J. High Energy Phys.* **2018**, *6*, 108, doi:10.1007/JHEP06(2018)108. [[CrossRef](#)]
21. Aaboud, M.; Aad, G.; Abbott, B.; Abdinov, O.; Abeloos, B.; Abidi, S.H.; AbouZeid, O.S.; Abraham, N.L.; Abramowicz, H.; Abreu, H.; et al. Search for dark matter produced in association with bottom or top quarks in $\sqrt{s} = 13$ TeV pp collisions with the ATLAS detector. *Eur. Phys. J.* **2018**, *C78*, 18, doi:10.1140/epjc/s10052-017-5486-1. [[CrossRef](#)]
22. Sirunyan, A.M.; CMS Collaboration. Search for narrow and broad dijet resonances in proton-proton collisions at $\sqrt{s} = 13$ TeV and constraints on dark matter mediators and other new particles. *J. High Energy Phys.* **2018**, *8*, 130, doi:10.1007/JHEP08(2018)130. [[CrossRef](#)]
23. Aaboud, M.; Aad, G.; Abbott, B.; Abdallah, J.; Abdinov, O.; Abeloos, B.; Abidi, S.H.; AbouZeid, O.S.; Abraham, N.L.; Abramowicz, H.; et al. Search for new phenomena in dijet events using 37 fb^{-1} of pp collision data collected at $\sqrt{s} = 13$ TeV with the ATLAS detector. *Phys. Rev. D* **2017**, *D96*, 052004, doi:10.1103/PhysRevD.96.052004. [[CrossRef](#)]
24. Aaboud, M.; Kupco, A.; Webb, S.; Dreyer, T.; Wang, Y.; Jakobs, K.; Spousta, M.; Cobal, M.; Wang, P.; Schmitt, S.; et al. Search for low-mass dijet resonances using trigger-level jets with the ATLAS detector in pp collisions at $\sqrt{s} = 13$ TeV. *Phys. Rev. Lett.* **2018**, *121*, 081801, doi:10.1103/PhysRevLett.121.081801. [[CrossRef](#)] [[PubMed](#)]
25. Sirunyan, A.M.; Tumasyan, A.; Adam, W.; Ambrogio, F.; Asilar, E.; Bergauer, T.; Brandstetter, J.; Brondolin, E.; Dragicevic, M.; Erö, J.; et al. Search for new physics in dijet angular distributions using proton-proton collisions at $\sqrt{s} = 13$ TeV and constraints on dark matter and other models. *arXiv* **2018**, arXiv:hep-ex/1803.08030.

26. Sirunyan, A.M.; Tumasyan, A.; Adam, W.; Ambrogio, F.; Asilar, E.; Bergauer, T.; Brandstetter, J.; Brondolin, E.; Dragicevic, M.; Erö, J.; et al. Search for low mass vector resonances decaying into quark-antiquark pairs in proton-proton collisions at $\sqrt{s} = 13$ TeV. *J. High Energy Phys.* **2018**, *1*, 097, doi:10.1007/JHEP01(2018)097. [[CrossRef](#)]
27. CMS EXO Summary Plots. Available online: <https://twiki.cern.ch/twiki/pub/CMSPublic/PhysicsResultsEXO/DM-summary-plots-Jul17.pdf> (accessed on 29 October 2018).
28. Elliot, A. Dark matter searches with the ATLAS detector. *EPJ Web Conf.* **2017**, *158*, 01007, doi:10.1051/epjconf/201715801007. [[CrossRef](#)]
29. Busoni, G.; Buchmueller, O.; Busoni, G.; D'Eramo, F.; De Roeck, A.; De Simone, A.; Doglioni, C.; Dolan, M.J.; Genest, M.H.; Hahn, K.; et al. Recommendations on presenting LHC searches for missing transverse energy signals using simplified s -channel models of dark matter. *arXiv* **2016**, arXiv:hep-ex/1603.04156.



© 2018 by the authors. Licensee MDPI, Basel, Switzerland. This article is an open access article distributed under the terms and conditions of the Creative Commons Attribution (CC BY) license (<http://creativecommons.org/licenses/by/4.0/>).